Iron Loss Calculation in Steel Laminations at High Frequencies

François Henrotte[1], Simon Steentjes[2], Kay Hameyer[2], and Christophe Geuzaine[3]

[1]IMMc, UCL, Louvain-la-Neuve B-1348, Belgium
[2]Institute of Electrical Machines, RWTH Aachen University, Aachen D-52056, Germany
[3]Department of Electrical Engineering and Computer Science, University of Liège, Liège B-4000, Belgium

This paper proposes a model for the computation of iron losses in steel laminations accounting simultaneously for magnetic hysteresis and eddy currents. The proposed model is well suited for finite element implementation and relies on a consistent thermodynamic background. The focus of this paper is particularly set on a systematic and accurate identification of material parameters from standard dc measurements (Epstein frame, single-sheet tester). Once identified, those material parameters can be used to obtain quantitative predictions of iron losses at higher frequencies and in the presence of higher harmonics. The model and the identification process are validated against measurements for a M235-35 A electrical steel over a wide range of field intensity and frequencies.

***Index Terms*—Electromagnetic modeling, finite element analysis, magnetic hysteresis, magnetic losses.**

I. Thermodynamic Foundation

THE hysteresis model advocated in this paper follows directly from the expression (1) of the conservation of energy:

$$\dot{u} = \mathbf{h} \cdot \dot{\mathbf{J}} - D \tag{1}$$

in terms of the energy density of the material u, the dissipation function D and the magnetic work $\mathbf{h} \cdot \dot{\mathbf{J}}$ [1]. Note that, for the sake of conciseness, the term $\mu_0 \mathbf{h}$ is disregarded in this presentation, so that the magnetic polarization $\mathbf{J}$ is assimilated with the flux density $\mathbf{b}$. A dot above a symbol stands for a total time derivative. The energy density u depends on $\mathbf{J}$ and its time derivative writes

$$\dot{u} = \mathbf{h}_r \cdot \dot{\mathbf{J}} \quad \text{with} \quad \mathbf{h}_r := \partial_{\mathbf{J}} u. \tag{2}$$

We call the field $\mathbf{h}_r$ reversible magnetic field because the magnetic work it delivers is fully converted into internal energy.

Magnetic hysteresis losses can be interpreted in terms of the mechanical analogy shown in Fig. 1 (left) [2], [3]. The physical origin of the dry friction force [4] represented by the slider is the pinning effect that opposes the motion of Bloch walls [5]. The corresponding dissipation function writes

$$D = \kappa |\dot{\mathbf{J}}| := \mathbf{h}_i \cdot \dot{\mathbf{J}} \tag{3}$$

in terms of the pinning field κ, which has the dimensions of a magnetic field. The field $\mathbf{h}_i$ is called irreversible magnetic field because the associated magnetic work is integrally dissipated. The functional (3) is not differentiable for $\dot{\mathbf{J}} = 0$ (therefore, one is not allowed to simply write $\mathbf{h}_i = \partial_{\dot{\mathbf{J}}} D$) but, as it is convex, one can write

$$\mathbf{h}_i \in \partial_{\dot{\mathbf{J}}} D \tag{4}$$

Manuscript received July 4, 2013; revised August 27, 2013; accepted September 15, 2013. Date of current version February 21, 2014. Corresponding author: F. Henrotte (e-mail: francois.henrotte@uclouvain.be).

Color versions of one or more of the figures in this paper are available online at http://ieeexplore.ieee.org.

Digital Object Identifier 10.1109/TMAG.2013.2282830

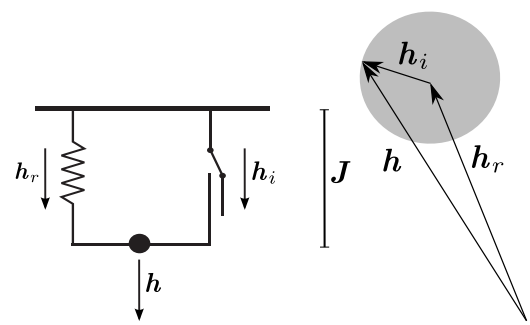

Fig. 1. Left: lumped parameter mechanical analogy for magnetic hysteresis as a nonlinear spring in parallel with a slider. Right: graphical representation of the vector (7). Gray circle: subgradient (5).

where the set

$$\partial_{\dot{\mathbf{J}}} D = \{\mathbf{h}_i, |\mathbf{h}_i| \le \kappa \text{ if } \dot{\mathbf{J}} = 0,\ \mathbf{h}_i = \kappa \mathbf{e}_{\dot{\mathbf{J}}} \text{ otherwise}\} \tag{5}$$

with $\mathbf{e}_{\mathbf{y}} := \mathbf{y}/|\mathbf{y}|$ the unit vector parallel to the vector $\mathbf{y}$, is the subgradient of the functional D.

A. Constitutive Relationships and Update Rule

The conservation of energy (1) now writes

$$(\mathbf{h} - \mathbf{h}_r - \mathbf{h}_i) \cdot \dot{\mathbf{J}} = 0 \qquad \forall \dot{\mathbf{J}}. \tag{6}$$

As the state variable $\mathbf{J}$ is arbitrary, the factor between the parenthesis must vanish and the governing relationship

$$\mathbf{h} - \mathbf{h}_r - \mathbf{h}_i = 0 \quad \Rightarrow \quad \mathbf{h} - \mathbf{h}_r \in \partial_{\dot{\mathbf{J}}} D \tag{7}$$

is obtained, where (2) and (4) have been used. This equation can be given a clear pictorial representation, see Fig. 1 (right). The gray sphere centered at $\mathbf{h}_r$ is the representation of the subgradient. Starting from the situation shown in Fig. 1, if the tip of applied magnetic field $\mathbf{h}$ enters the sphere, the reversible magnetic component $\mathbf{h}_r$ is not modified, which means that no change in the magnetic polarization occurs either, $\dot{\mathbf{J}} = 0$. Both $\mathbf{h}_r$ and $\mathbf{J}$, which are in a 1–1 relationship, remain

unmodified as long as the tip of $\mathbf{h}$ remains inside the sphere. If now $\mathbf{h}$ tends to reach out of the sphere, which is forbidden by the condition (7), the sphere must be shifted. The magnetic polarization changes in this case, $\dot{\mathbf{J}} \neq 0$, and the evolution of $\mathbf{h}_r$ is ruled by

$$\mathbf{h} = \mathbf{h}_r + \kappa\ \mathbf{e}_{\dot{\mathbf{J}}} \tag{8}$$

obtained from (7) and (5). Defining the susceptibility tensor $\underline{\chi}(\mathbf{h}_r)$ by $\dot{\mathbf{J}} = (\partial_{\mathbf{h}_r}\mathbf{J}) \cdot \dot{\mathbf{h}}_r := \underline{\chi}(\mathbf{h}_r) \cdot \dot{\mathbf{h}}_r$, it appears that (8) is an implicit and nonlinear differential equation in $\mathbf{h}_r$. Its exact solution might be rather delicate but an approximate solution can be obtained readily with the explicit update rule

$$\mathbf{h}_r = \mathcal{U}(\mathbf{h}, \mathbf{h}_r^{(p)}, \kappa) := \begin{cases} \mathbf{h} - \kappa \frac{\mathbf{h}-\mathbf{h}_r^{(p)}}{|\mathbf{h}-\mathbf{h}_r^{(p)}|}, & \text{if } |\mathbf{h} - \mathbf{h}_r^{(p)}| \geq \kappa \\ \mathbf{h}_r, & \text{otherwise} \end{cases} \tag{9}$$

where the exponent (p) indicates a quantity evaluated at the previous time step. The update rule (9) is exact in all situations, where $\dot{\mathbf{J}} \,//\, \dot{\mathbf{h}}_r$, i.e., in unidirectional problems (which is the case in experimental setups [9]), in the linear part of the magnetic curve and in case of rotational hysteresis. In all other situations, the simplified rule is an approximation. An alternative approach based on the minimization of a pseudopotential [1] allows obtaining an exact solution of (9) in all the cases. It should be noted that the conditional statement in (9) is the whole implementation of the concept of subgradient.

B. Saturation Characteristic

Assuming an isotropic material, the vectors $\mathbf{J}$ and $\mathbf{h}_r$ are colinear and one has

$$\mathbf{J} := J_{\text{an}}(|\,\mathbf{h}_r|)\ \mathbf{e}_{\mathbf{h}_r} \tag{10}$$

with J_{an} the anhysteretic magnetization curve, which is scalar and one-to-one. Note that we do not account for the additional $\mu_0 h$ term in our definition of the anhysteretic curve, as it is usually compensated in Epstein frame measurements. Experience shows that anhysteretic curves can be represented accurately by a double Langevin function [2]

$$J_{\text{an}}(h_r) := J_a L\left(\frac{h_r}{h_a}\right) + J_b L\left(\frac{h_r}{h_b}\right) \tag{11}$$

with $L(x) = \coth x - (1/x)$. The term indexed with a b represents the magnetic polarization due to the motion of Bloch walls whereas the term indexed with an a represents the magnetic polarization, occurring at high field intensity that is associated with the rotation of the magnetic moments relative to their preferred easy-magnetization axis.

II. Two-Scale Model

In reality, the pinning field κ cannot be represented by a single constant, but obeys a distribution law. First, we show how to account for this distribution in the theory using a two-scale approach, leaving it for the following section to discuss how the distribution can be identified from measurements.

The idea of the two-scale approach is to decompose the material sample into independent abstract regions, all subjected to the magnetic field $\mathbf{h}$, but characterized each by a particular value κ of the pinning field. Let $\omega(\kappa)$ be the probability that a magnetic moment belongs to the region with pinning field κ. The magnetic state of the κ-region is described by a magnetic polarization $\mathbf{J}^\star(\kappa)$. It is linked to the reversible magnetic field $\mathbf{h}_r^\star(\kappa)$ by the constitutive relationship

$$\mathbf{J}^\star(\kappa) = \omega(\kappa)\ \mathbf{J}_{\text{an}}(h_r^\star(\kappa)) \tag{12}$$

and one has in each region an evolution equation

$$\mathbf{h} = \mathbf{h}_r^\star(\kappa) + \kappa\ \mathbf{e}_{\dot{\mathbf{J}}^\star(\kappa)} \tag{13}$$

built on the same model as (8).

Knowing the magnetic field $\mathbf{h}$, the problem can thus be solved independently in each κ-region. It remains to average out region-based quantities into the homogenized macroscopic quantities that will be used in the finite element (FE) formulation. The homogenized magnetic polarization is naturally defined as

$$\mathbf{J} = \int_0^\infty \mathbf{J}^\star(\kappa)\ \mathrm{d}\kappa \tag{14}$$

and the homogenized energy balance

$$0 = \textstyle\int_0^\infty \omega(\kappa)\ \left(\mathbf{h} - \mathbf{h}_r^\star(\kappa) - \mathbf{h}_i^\star(\kappa)\right) \cdot \dot{\mathbf{J}}\ \mathrm{d}\kappa$$

which is verified if the local equations (13) are verified, defines the homogenized reversible magnetic field

$$\mathbf{h}_r = \int_0^\infty \omega(\kappa)\ \mathbf{h}_r^\star(\kappa)\ \mathrm{d}\kappa. \tag{15}$$

III. Identification of Material Parameters

In this model, the memory of the material (memory effect) is represented by the values of the vectors $\mathbf{h}_r^\star(\kappa)$, the demagnetized state (wiped-out memory state) being the state with $\mathbf{h}^\star(\kappa) = 0, \forall\kappa$. The purpose of this section is to show how the distribution $\omega(\kappa)$ can be identified from standard Epstein measurements. As the loading is always unidirectional in such measurements, we shall work throughout this section with the modulus of the field $h := |\mathbf{h}|$.

Starting from the demagnetized stated, a unidirectional magnetic loading until $h = h_A$ is first considered. The κ-regions involved in this loading are those such that $\kappa < h_A$ and one has, at the end, $h_r(\kappa) = h_A - \kappa$, the other $h_r(\kappa)$ remaining zero. The homogenized reversible field is then

$$h_r(0 \to h_A) = \int_0^\infty \max(h_A - \kappa, 0)\ \omega(\kappa)\ d\kappa = F(h_A)$$

with the definition of the auxiliary function

$$F(h) := \int_0^h \omega(\kappa)\ (h - \kappa)\ \mathrm{d}\kappa \tag{16}$$

whose first and second derivatives are, respectively

$$\partial_h F(h) = \int_0^h \omega(\kappa)\ \mathrm{d}\kappa, \quad \partial_h^2 F(h) = \omega(h). \tag{17}$$

Starting over now from this state, the material is unloaded until the magnetic field reaches $h_B < h_A$, always in the same direction. The κ-regions involved in the unloading are those such that $h_B + \kappa < h_A - \kappa$, i.e., $\kappa < (h_A - h_B)/2$. After some

algebra, the homogenized reversible field at the end of the loading–unloading process can be shown to be

$$h_r(0 \to h_A \to h_B) = F(h_A) - 2F\left(\frac{h_A - h_B}{2}\right). \quad (18)$$

The auxiliary function F plays, as one observes, a central role. Its second derivative is the sought distribution $\omega(\kappa)$, so, if we can identify F, ω is also identified in principle. The virgin curve of the material (first magnetization curve) is also simply the composition of the anhysteretic curve with F

$$J_{\text{virgin}}(h) = J_{\text{an}}(h_r(0 \to h)) = J_{\text{an}}(F(h)). \quad (19)$$

Given the anhysteretic curve, the latter relation could serve as a basis for the identification of F. However, the measurement of the anhysteretic curve is not part of standard magnetic measurement setups. Therefore, an identification strategy independent of J_{an} has been preferred that relies on the coercive fields $h_c(h)$ of symmetrical hysteresis loops. The coercive field of a loop of magnitude h is indeed characterized by

$$J_{\text{an}}(h_r(0 \to h \to -h_c)) = 0 \quad (20)$$

which implies

$$F(h) - 2F\left(\frac{h + h_c(h)}{2}\right) = 0. \quad (21)$$

The $h_c(h)$ characteristic is obtained from the measurement of a series of hysteresis loop of increasing amplitude. It has the following properties: 1) $h_c(0) = 0$; 2) $\exists h_s, h_c(h) = h_{c\max}\ \forall h > h_s$; and 3) $h_c(h) < h$. They turn out to be sufficient to completely identify the function F. Indeed, 1) tells that $F(0) = 0$. From 2), one observes that $F(h) = h - h_{c\max}, \forall h > h_s$. Finally, 3) implies that the series defined by $x^n = (x^{n-1} + h_c(x^{n-1}))/2 < x^{n-1}$ is strictly decreasing. Starting from an arbitrary initial value $x^0 > h_s$, for which it is known that $F(x^0) = x^0 - h_{c\max}$, the value of F for all subsequent terms of the series is recursively given by $F(x^n) = F(x^{n-1})/2$. Clearly, the series converges toward $F(0) = 0$. Several initial values x_0 can be selected until a sufficiently fine representation of F is obtained. We have used four series, initialized with $x_0 = \{1, 1.25, 1.5, \text{and } 1.75\}h_s$, with $h_s = 500$ A/m.

The identification procedure described above has been applied to five non grain-oriented steel grades, namely, M235-35A (3.2 wt% Si), M250-35A (3.2 wt% Si), M330-35A (2.4 wt% Si), M330-50A (2.4 wt% Si), and M400-50A (2.4 wt% Si). The measured coercive field characteristics $h_c(h)$ are shown in Fig. 2. The corresponding F functions, Fig. 3, have all the same asymptotic behavior at high field with unitary slope, whereas the inset compares the behavior at low field in logarithmic scale.

The pinning field distribution $\omega(\kappa)$ is the second derivative of F. As numerical differentiation is extremely inaccurate and should therefore be avoided, the function F is first matched with a two times differentiable analytic function. After differentiation, the pinning field distributions are obtained, see Fig. 4. The behavior of the distribution $\omega(\kappa \to 0)$ is very sensitive to the representation of the measured characteristic $h_c(h)$. As the latter is represented piecewise linear, it behaves

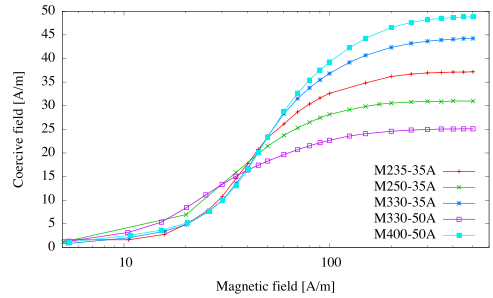

Fig. 2. Coercive field $h_c(h)$ of symmetrical hysteresis loops measured for five different steel grades. All measurement points are represented.

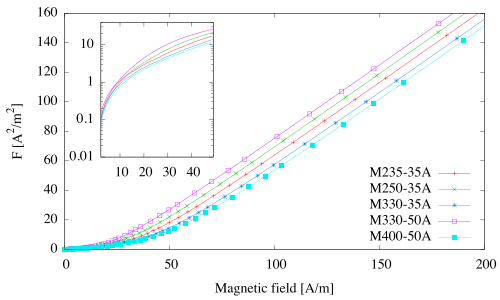

Fig. 3. Identified F functions for five different steel grades. The behavior at low field is detailed in the inset in logarithmic scale.

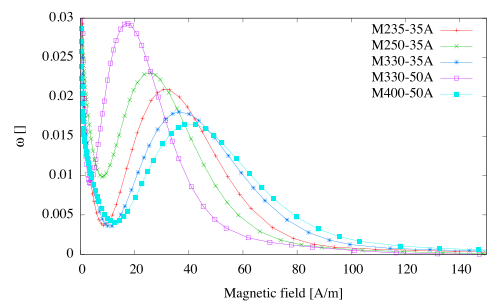

Fig. 4. Identified pinning field distribution $\omega(\kappa)$ for five different steel grades.

linearly when $h \to 0$, which is not necessarily true from a theoretical point of view. However, without a true theory to establish the asymptotic behavior of $h_c(h)$ and $\omega(\kappa)$ at low fields, it was decided not to modify the measured data and to acknowledge distributions $\omega(\kappa)$ with a peak at zero.

Each grade has its own characteristic distribution $\omega(\kappa)$, which can in principle be traced back to objective differences in the lamination thickness and in the microstructure. For instance, M235-35A and M250-35A, have the same alloy and same thickness but different grain sizes. M330-35A and M330-50A have also the same alloy, but different grain sizes and different thickness. The identified pinning field distribution reveals thus useful correlations between the macroscopic behavior of the material and its composition and microstructure.

Finally, once the function F is known for a material, the four parameters of the double Langevin representation (11) $J_{\text{an}}(h)$ can be determined by matching the measured virgin curve $J_{\text{virgin}}(h)$ with $J_{\text{an}}(F(h))$.

IV. Finite Element Implementation

For the FE implementation, a discrete approximation of the continuous distribution $\omega(\kappa)$ is needed. It is obtained by

partitioning the magnetic field range into n regions determined by selected values $h^0 = 0 < h^1 < \cdots < h^{n-1} < h^n = \infty$ of the magnetic field. One has then, for $k = 1, \ldots, n$

$$\omega^k = \int_{h^{k-1}}^{h^k} \omega(\kappa)\ \mathrm{d}\kappa = \partial_h F(h^k) - \partial_h F(h^{k-1}) \tag{22}$$

$$\kappa^k = \frac{\int_{h^{k-1}}^{h^k} \omega(\kappa)\ \kappa\ \mathrm{d}\kappa}{\int_{h^{k-1}}^{h^k} \omega(\kappa)\ \mathrm{d}\kappa} = \frac{[h\ \partial_h F(h) - F(h)]_{h^{k-1}}^{h^k}}{\omega^k}. \tag{23}$$

Clearly, $\sum_{k=1}^n \omega^k = 1$ and, if $n = 1$, $\omega^1 = 1$ and $\kappa^1 = h_{c\max}$. The integrals of Section II become sums and the homogenization relations (14) and (15) write

$$\mathbf{J} = \sum_{k=1}^n \mathbf{J}^k, \quad \mathbf{h}_r = \sum_{k=1}^n \omega^k\ \mathbf{h}_r^k \tag{24}$$

with $\mathbf{J}^k$ and $\mathbf{h}_r^k$ the magnetic polarization and the reversible magnetic field of region k. This amounts to connect in series n cells like the one shown in Fig. 1, each cell having its own value κ^k of the pinning field. The update rule (9) is used for each cell after substituting κ with κ^k and $\mathbf{h}_r$ with $\mathbf{h}_r^k$.

As the magnetic field is the natural driving quantity for the irreversible constitutive relationship (7), problems with hysteresis are naturally solved with a h-field formulation. The weak formulation of Faraday's law reads

$$\int_\Omega \left(\dot{\mathbf{b}} \cdot \mathbf{h}' + \sigma^{-1} \mathrm{curl}\, \mathbf{h} \cdot \mathrm{curl}\, \mathbf{h}'\right) d\Omega = 0 \quad \forall \mathbf{h}' \in \mathcal{H} \tag{25}$$

with $\mathcal{H}$ an appropriate functional space fulfilling Dirichlet boundary conditions.

Practically, the anhysteretic curve is represented in the FE implementation as a curve giving the magnetic susceptibility $\chi := J/h_r$ as a function of $|\mathbf{h}_r|^2$, with $\mathbf{h}_r$ defined by (14). The induction field is then

$$\mathbf{b}(\mathbf{h}, \mathbf{h}_r) = \mu_0 \mathbf{h} + \chi(|\mathbf{h}_r|^2)\ \mathbf{h}_r \tag{26}$$

and its time derivative in terms of the unknown $\mathbf{h}$ writes (note the dyadic product $\mathbf{h}_r \mathbf{h}_r$)

$$\dot{\mathbf{b}}(\mathbf{h}, \mathbf{h}_r) = \left(\mu_0 + \left(\chi(|\mathbf{h}_r|^2)\mathbb{I} + 2\dot{\chi}(|\mathbf{h}_r|^2)\ \mathbf{h}_r \mathbf{h}_r\right) \partial_{\mathbf{h}} \mathbf{h}_r\right) \dot{\mathbf{h}}$$

where $\mathbb{I}$ is the identity matrix and the tensor $\partial_{\mathbf{h}} \mathbf{h}_r$ is expressed by derivation of the update rule (9)

$$\partial_{\mathbf{h}} \mathbf{h}_r = \sum_{k=1}^n \omega^k\ \partial_{\mathbf{h}} \mathbf{h}_r^k = \sum_{k=1}^n \omega^k\ \partial_{\mathbf{h}} \mathcal{U}\left(\mathbf{h}, \mathbf{h}_r^{k(p)}, \kappa^k\right). \tag{27}$$

V. Validation

Standard electric steel lamination measurements are obtained under sinusoidal $\langle \mathbf{b} \rangle$-field conditions. To identify them with FE simulations, the applied $\mathbf{h}$-field that yields a sinusoidal flux through the lamination must be determined. This is done iteratively. Simulations were done with an electric conductivity $\sigma = 1.57 \cdot 10^6\ \Omega\mathrm{m}^{-1} (\rho = 63.7\ \mu\Omega\mathrm{cm})$. A very good match over a large range of field intensities (up to 1.6 T) and frequencies (up to 400 Hz) is observed, see Fig. 5. It is remarkable that the large amount of measured data can be quantitatively reproduced with so few parameters. This indicates that the physical model based on the dry friction analogy is close enough to the reality.

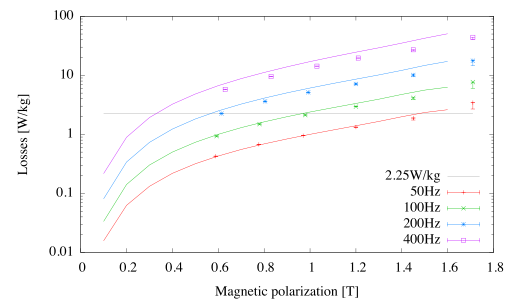

Fig. 5. Comparison between measured data for M23535A at 50, 100, 200, and 400 Hz (solid lines) and calculated data (points).

The identified parameters fully characterize the material, irrespective of load and geometry. They can be used in 2-D or 3-D models, or to calculate iron losses under loads for which measurements are hard to obtain or unavailable, in particular at higher frequencies and in the presence of higher harmonics. In a second time, the loss model could be coupled with the modeling of macroscopic devices (e.g., electrical machines) using, e.g., of a homogenization approach like the one proposed in [10].

Acknowledgment

This work was supported in part by the Belgian Science Policy under Grant IAP P7/02, in part by the Belgian French Community under Grant ARC 09/14-02, and in part by Walloon Region under WBGreen Project FEDO. The work of S. Steentjes was supported by the Deutsche Forschungsgemeinschaft through Project Improved modelling and characterisation of ferromagnetic materials and their losses.

References

[1] V. François-Lavet, F. Henrotte, L. Stainier, L. Noels, and C. Geuzaine, "An energy-based variational model of ferromagnetic hysteresis for finite element computations," *J. Comput. Appl. Math.*, vol. 246, pp. 243–250, Jul. 2013.

[2] F. Henrotte, A. Nicolet, and K. Hameyer, "An energy-based vector hysteresis model for ferromagnetic materials," *Int. J. Comput. Math. Electr. Electron. Eng.*, vol. 25, no. 1, pp. 71–80, 2006.

[3] F. Henrotte and K. Hameyer, "A dynamical vector hysteresis model based on an energy approach," *IEEE Trans. Magn.*, vol. 42, no. 4, pp. 899–902, Apr. 2006.

[4] A. Bergqvist, "Magnetic vector hysteresis model with dry friction-like pinning," *Phys. B, Condensed Matter*, vol. 233, no. 4, pp. 342–347, 1997.

[5] G. Bertotti, *Hysteresis in Magnetism*. San Francisco, CA, USA: Academic, 1998.

[6] I. Mayergoyz, *Mathematical Models of Hysteresis and Their Applications*, 2nd ed. San Francisco, CA, USA: Academic, 2003.

[7] D. C. Jiles and D. L. Atherton, "Theory of ferromagnetic hysteresis," *J. Magn. Magn. Mater.*, vol. 61, nos. 1–2, pp. 48–60, 1986.

[8] G. Bertotti, "Connection between microstructure and magnetic properties of soft magnetic materials," *J. Magn. Magn. Mater.*, vol. 320, no. 20, pp. 2436–2442, 2008.

[9] *Magnetic Materials: Part 2: Methods of Measurement of the Magnetic Properties of Electrical Steel Strip and Sheet by Means of an Epstein Frame*, IEC Standard 60404-2:1996 + A1:2008, 2008.

[10] I. Niyonzima, R. V. Sabariego, P. Dular, F. Henrotte, and C. Geuzaine, "Computational homogenization for laminated ferromagnetic cores in magnetodynamics," *IEEE Trans. Magn.*, vol. 49, no. 5, pp. 2049–2052, May 2013.